

Thermal diode effect detected in allosteric communication pathways of PDZ-2 protein. A computational study.

Germán A. Miño-Galaz^{1,2,3}

¹Group of Nanomaterials. www.gnm.cl
Departamento de Física, Facultad de Ciencias, Universidad de Chile
Las Palmeras 3425, Ñuñoa, Santiago de Chile
(germino@u.uchile.cl,
german.mino.galaz@gmail.com)

²Centro Interdisciplinario de Neurociencias de Valparaíso (CINV), Universidad de Valparaíso, Valparaíso, Chile

³Center for Bioinformatics and Integrative Biology (CBIB), Facultad en Ciencias Biologicas, Universidad Andres Bello, Santiago, Chile

Abstract

Allosteric communication in proteins is a central and yet not solved problem of structural biochemistry. Molecular communication in proteins requires the existence of allosteric pathways. Previous findings, from computational biology (Ota and Agard, 2005), has proposed that heat diffuses in a protein through allosteric pathways. In this work we studied heat diffusion in the well know PDZ-2 protein. This protein has two cognate allosteric pathways and we confirm that heat flows preferentially through them. Also, a new property is observed for protein structures: heat diffuses asymmetrically through them. The underling structure of this asymmetrical heat flow is the hydrogen bond of normal length ($\sim 2.85 \text{ \AA}$), that can act as a thermal diode. Also asymmetrical heat diffusion is due, in a higher scale, to local structural organization of residues. This asymmetrical energy flow may be relevant for allosteric signal communication directionality in protein structures.

Introduction

Signal transmission through protein structures can occur and be functionally relevant. It depends on the structural or dynamical connectivity in short (3 Å) or long distances (100 Å), and the sites connected by this signal are known as allosteric sites. Thus, allosteric communication in proteins is a central problem in structural biochemistry. This phenomena is involved in crucial cellular and physiological functions and is determinant in human diseases (Laine et al., 2012. Noinaj et al., 2011. Seldeen et al., 2011). In the most simple cases, allosteric communication involves a protein, a ligand site and an effector site in the same protein. After ligand binding, a signal is propagated throughout the protein structure to the effector site. Depending on the effect of the signal on the effector site, the allosterism may be positive or negative (Voet and Voet, 1995). For example, as a case of positive modulation, the binding of vancomycin to the glycopeptide antibiotics facilitates the dimerization of two molecules of the antibiotic (Jusuf et al., 2003). On the other side, a negative modulation is observed in the binding of the cAMP molecules to the catabolite activator protein (CAP). Here binding of the first cAMP molecule difficult the binding of the second cAMP to CAP (Popovych et al., 2006).

Signal propagation through protein structures may have diverse origins, and might not be associated with any discernible structural change. For example, signal propagation in protein structures were correlated with paths of energy flow (Ota et al., 2005. Fuentes et al., 2006. Ma et al., 2012. Sharp et al., 2006. Leitner, 2008). Velocities of energy propagation of the order of 10 Å ps^{-1} (Leitner, 2008) were observed, and the dependence of allosteric pathways with the frequency of normal modes vibration of mioglobin have been reported (Leitner et al., 2009). From the physical point of view allosteric energy flow in proteins mimics in many ways transport on percolation networks with fractal dimension of ~ 2.5 . A characteristic of energy flow in percolation clusters is that energy flows anisotropically, that is, fast along channels physically connected

and otherwise slow along numerous pathways reaching death ends (Letiner, 2008).

Thermodynamically, the free energy of allosteric processes in proteins has been interpreted by attributing the enthalpic part to conformational changes in the protein structure and the entropic contribution to the variability in the dynamical fluctuations of residues (Tsai et al., 2008. Cooper et al., 1984, Fuentes et al., 2006). Based in this distinction, three types of allosteric signaling are distinguished: Type I, with small conformational changes, governed largely by entropy ($\Delta H \approx 0$); Type II with the participation of the enthalpic and entropic components in different extents; and Type III largely governed by enthalpic changes ($\Delta S \approx 0$) (Tsai et al., 2008). Type I allosteric communication has been less studied with respect the enthalpic communication of the Types II and III (Monod et al., 1965. Koshland et al., 1966). Type I allosterism, also know as dynamic or configurational allosterism, was initially proposed by Cooper and Dryden in 1984. According to these authors the effect arises from changes in frequencies and amplitudes of macromolecular fluctuations around the same conformation of a protein and involve several forms of dynamic behavior, ranging from highly correlated, low-frequency normal-mode vibrations to random local anharmonic motions of individual groups or atoms. These fluctuations can be described in therms of vibration, libration, or rotation of individual groups that propagate vibrational energy along the protein structure (Cooper et al., 1894). Systems as staphylococcal nuclease (Green et al., 1993), myoglobin (Frauenfelder et al., 2001), serine proteases (Mace et al., 1995), HIV-1 protease (Olsen et al., 1999), dihydrofolate reductase (Rod et al., 2003), β -lactamase (Meroueh et al., 2002) and the Post synaptic density-95/Drosophila disc/Zonula occludens-1 (PDZ) domain protein family (Lockless et al., 1999) are known to transfer allosteric information by changes in their dynamics without significant conformational changes (Type I allosterism).

The allosteric pathways of the PDZ domain family, in particular, are very interesting for involving residues which are far in terms of the protein structure. The PDZ protein family have a common structural domain of 80-96 amino-acids,

and appears in signaling proteins of bacteria, yeast, plants, viruses (Boxus et al., 2008) and animals (Ponting et al., 1997). Experimental (Fuentes et al., 2006) , statistical coupling analysis (SCA) (Lockless et al., 1999) and theoretical models (Erman, 2011) models has been used to characterize this protein family, and a consensus of its allosteric pathways has been reached. In particular, using cross-correlation analysis, Kong and Karplus (2009) report two pathways of allosteric communication for PDZ-2. In Pathway I (See Figure 1) the allosteric communication pathway goes from strand β_2 (residues 19-24) and extends along the long axis of the helix α_1 (residues 44-49) and Pathway II starts at strand β_2 and goes across strands β_3 (residues 33-40), β_4 (residues 56-61), β_6 (residues 83-90) to β_1 (residues 6-13).

A structural interpretation for the correlations obtained by SCA was obtained using a non-equilibrium molecular dynamics (MD) simulation technique known as Anisotropic Thermal Diffusion (ATD) (Ota et al., 2005). ATD is a MD pump-probe method that has been used to study of allosteric communication pathways in proteins (Burendahl and Nilsson, 2012; Liu et al. 2013). In its original formulation the protein model is equilibrated in absence of solvent at very low temperature to minimize background noise. After that, a specific residue is heated by the coupling of a thermal bath (pump) and the increase in vibrational energy is measured in different sites of the protein (probe) in a short subsequent lapse of time. The pathways of energetic connectivity observed with ATD were consistent with the correlations between residues found by SCA (Ota et al., 2005). The correlations between anisotropic vibrational energy propagation and allostereism has been confirmed experimentally (Liu et al, 2013), supporting the utility of ATD for the comprehension of these mechanisms.

The ATD method is fast and can be extended to the automatic mapping of the heat propagation from every residue of a structure to every other residue (Martínez et al, 2011). Here, we review the pathways of heat propagation of the PDZ-2 protein comprehensively and obtain full heat propagation maps of energetic connectivity. We confirm that vibrational energy flows through the

connectivity network though allosteric pathways previously reported (Kong and Karplus, 1999) but, in addition, we show that these paths of energetic connectivity are not symmetric. This means that vibrational perturbations (and, thus, the allosteric signal) flows through directional paths. Here we show that asymmetrical heat diffusion occurs in hydrogen bonds of normal length (~ 2.85 Å) that operate as thermal diodes. In contrast the thermal diode effect seems to be suppressed in short hydrogen bonds (~ 2.60 Å), giving rise to symmetrical thermal diffusion. Another source of asymmetrical heat diffusion is due, in a higher scale, to local structural organization of residues. This asymmetrical energy flow may be relevant for allosteric signal communication directionality in protein structures.

Methods and Computational details.

The PDZ-2 protein in presence of ligand, from now PDZ-2·L (PDB ID: 1D5G), and without ligand, from now PDZ-2 (PDB ID: 3PDZ), were used for the simulations. These models are minimized and equilibrated using periodic boundary conditions at 298 K and 1 atm with water as explicit solvent and NaCl at 0.15 M. Constant temperature conditions were used through Langevin dynamics with a damping coefficient of 5 ps^{-1} . An integration time step of 1 fs was used and a cutoff of non-bonded forces at 12 Å with a switching function starting at 10 Å. The equilibration is divided in three steps. First, the coordinates of the protein models were fixed to allow the solvent and ions equilibrate for 200 ps. Second, the coordinates of the lateral chains were released and equilibrated for another 200 ps. Third, the all atoms were released and allowed to equilibrate for 2 ns. Finally, a production run of 20 ns was performed, after which, 20 equally spaced frames are selected for the ATD procedure. For each of the 20 frames, the solvent was removed and the protein model was cooled to 10 K for 100 ps MD. At this point the ATD procedure is applied using a set of automated scripts available at <https://leandro.iqm.unicamp.br/atd-scripts> (Martínez et al, 2011). The scripts allow the automated heating of each residue of protein

individually, and the analysis of the temperature of each other residue after a short predefined time-lapse, which is set to 30 ps (Martínez et al, 2011). Each residue is individually coupled to a thermal bath at 300 K and the thermal response in the rest of the protein is recovered. Here, 20 independent ATD scanning are performed for PDZ-2 and PDZ-2·L. The results of the scans were averaged and give rise to contact and thermal diffusion maps shown in Figure 2. All simulations were performed by use of NAMD2.9 software (Kale et al. 1999) using the CHARMM22 potential with CMAP correction (Mackerell et al. 1998). Visualization and data analysis were performed by use of VMD 1.8.7 software (Humphrey et al. 1996).

Results.

Figures 1 (a) and (b) show the structures of PDZ-2 and PDZ-2·L cases. Figure 2 (a) and (b) show the contact and thermal diffusion maps averaged for 20 independent simulations for both cases. The thermal diffusion maps show a rough similarity with the connectivity maps. Those plots show that the heat diffuses mainly by governed by the connectivity of the structure. This contacts belong to the covalent network of the primary structure or arise from the side-chain interactions of residues in different elements of the secondary structure of the models. The thermal maps show that the allocation of the allosteric pathways I and II for both models can be recovered using ATD. Both pathways can be deduced by inspection the averaged thermal maps. For pathway II we enter in Figure 2 in the abscissa of the thermal map for PDZ-2 at β_2 and we note thermal the coupling to β_3 (Box 1). Next, entering at the thermal map in the abscissa in β_3 we see the vibrational coupling with β_4 (Box 2). Then, entering at the thermal map of abscissa at β_4 we observe a vibrational coupling with β_6 (Box 3). Finally, by entering in the abscissa at β_6 we observe a strong vibrational coupling to β_1 (Box 4). With this inspection we note that the pathway II (Kong and Karplus, 2009) is recovered. Now In order to recover pathway I we look at PDZ-2·L thermal map. By entering in the abscissa at β_2 we observe a vibrational coupling with α_1 .

(encircled area). In the case PDZ-2 do not observe a strong coupling among β_2 and α_1 . Thus, the presence of ligand enhances this pathway. This can be clearly observed by comparison of both thermal maps.

Vibrational couplings are affected in other regions by the presence of ligand. The thermal map of PDZ-2 at abscissa in β_3 displays a strong vibrational coupling to residues 66 to 69 (a region between β_5 and α_2) and to residue 90 of to β_6 . Both these thermal coupling are quenched in the presence of ligand. Therefore, heat propagation, again, can be modulated by the presence of the ligand. This modulation results from structural rearrangements that can be observed, but are not at all clear, from the observation of contact maps alone. The similarity between contact maps and thermal maps suggest that communication pathways in Type I allosteric systems is primarily defined by atomic connectivity and its respective interaction. In this particular system, PDZ-2, the connectivity occurs among secondary structure elements of the protein.

The structural features that give rise to the most important energetic couplings was analyzed in detail. For example, the thermal maps in Figs. 2A and 2b display a thermal coupling between β_2 and His71, that belong to α_2 (highlighted with a triangle in thermal maps). This coupling arises from alternating hydrogen bonds (HB) between N δ 1 or N ϵ 2 of His71 with O γ 1 or with the oxygen atom of C=O backbone moiety of Thr23 in the ligand-free PDZ-2 model (Figure 3c). This effect is also observed in the thermal map of PDZ-2·L. In this case the heat transference between β_2 and α_2 is also due to formation of HB but now occurs between N δ 1 of His71 and oxygen atom of C=O backbone moiety of Gly24 or between N ϵ 2 of His71 and O γ 1 of Thr23 (Figure 3d). These observations are consistent with recent reports about the role of HB in heat diffusion in protein structures (Miño 2014, Zang, 2014)

Further observation of the results presented in Figure 2 reveals interesting features of heat propagation. Asymmetries are observed in the thermal diffusion maps. This can be qualitatively observed using the color scale of the thermal maps in Figure 2. For instance, in pathway II, the heat interchange between β_6 and β_1 is not symmetrical (observed in both PDZ-2 PDZ-2·L) or, in pathway I, the

heat interchange between β_2 and α_1 is not symmetrical (observed in PDZ-2-L) and we might suspect that there is a preferential directionality in those cases. In other points in the averaged thermal maps these asymmetries are observed and support the idea of directionality of signal propagation in allosteric pathways. These asymmetries can be rationalized by analysis of structure, pump-probe plots and energetic flow as is shown in the following cases.

At this point we pay attention to the asymmetrical interaction between Asp5 and Lys91 which are located in β_6 and β_1 , respectively of the PDZ-2 case. These two residues interact by a backbone hydrogen bond (Figure 4a). A clear asymmetrical pump-probe relationship is observed in figure 4b (circles), in which the heat is transferred with a preferential directionality going from Lys91 towards Asp5. In the 20 propagations (see methods section), 63% of the time those residues interact through one backbone hydrogen bond, 4.5% of the time interact between hydrogen bonds formed by their lateral chains and 36.5% of the time no interaction is observed (distances higher than 3.5 Å). The pump-probe profile with standard deviation is shown in figure 4c and reveals a response at Asp5 of 98.4 ± 15.9 K when the pump is applied to Lys91; and a response at Lys91 of 72.5 ± 12.3 K when the pump is applied to Asp5. These facts, plus the structural inspection of this hydrogen bond interaction suggest that the preferential directionality of the heat flow (Lys91 \rightarrow Asp5) is due to the spatial orientation of the hydrogen bond, that in this case has the configuration Lys91-N-H \cdots O=C-Asp5 (figure 4a, right). To evaluate the possible relationship between heat flow directionality and orientation of the hydrogen bond, the kinetic energy in time, of the atoms involved in this hydrogen bond was determined and is shown for three heat diffusion trajectories (figures 4d, e and f). As can be observed in Figure 4d, when the pump is applied to Lys91 a kinetic energy of ~ 1000 J/mol is observed at 10000 fs for the oxygen atom of the C=O moiety of Asp5. Inversely, when the pump is applied to Asp5 a kinetic energy of ~ 750 J/mol at 10000 fs is observed for the Nitrogen atom of the N-H moiety of Lys91. The same observation holds for the three depicted trajectories in which the C=O moiety consistently reports increased kinetic energy along the propagations. Those results imply that, in for this particular

configuration the hydrogen bond, the heat diffuses easily in the direction $\text{N-H} \rightarrow \text{O=C}$, and with difficulty in the inverse direction, $\text{N-H} \leftarrow \text{C=O}$. The origin of this effect may be due to the structural asymmetry of the hydrogen-bond and to the consequent stretching force constants associated to the N-H and C=O bonds (Figure 4a, right). For N-H and C=O the stretching force constant are 440 and 620 $\text{kcal}\cdot\text{mol}^{-1}\cdot\text{\AA}^{-2}$, respectively. Physically, this facilitates a wider oscillation of N-H with respect C=O. When the N-H moiety is excited, easily knock the O atom of the HB, readily transferring kinetic energy to it. The inverse is observed for C=O. When this moiety is excited, the O atom experience a restricted oscillation that is translated to a lower possibilities of knocking the H atom of the HB, and then a lower rate of heating is observed. Based on those observations we suggest that, for this specific case (a normal and nearly linear hydrogen bond), the hydrogen bond acts as a thermal diode, that is, can act as molecular motif that transfer thermal energy with a preferential directionality. This phenomena is not new, and have been observed in the hydrogen-bond enhanced thermal energy transport at functionalized, hydrophobic and hydrophilic silica–water interfaces. (Schoen, 2009). Nevertheless it is the first time, to our knowledge, that is reported in protein structures. For the PDZ-2·L case a similar observation are obtained for the analysis of the interaction between Asp5-Lys9 but due the presence of a higher percentage of interaction through lateral chains for the PDZ-2·L we restrict our presentation, at this point, for PDZ-2 case only.

As contrast, in a case of symmetrical heat diffusion, we pay attention to the structural arrangement Glu10-His86-Glu8 for PDZ-2 case. This arrangement interact through two hydrogen bonds as is depicted in figure 5a. In this specific case hydrogen bonds are intermittently formed between the available proton donors located at His86 (atoms N δ 1 and N ϵ 2) and the respective proton acceptors (Atoms O ϵ 1 and O ϵ 2) located at carboxylic moieties of the Glu10 and Glu8 residues. In the 20 propagations >95% of the cases these interaction is detected. A symmetrical pump-probe relation is observed in the interaction of Glu10-His86 and His86-Glu8 (rectangle figure 5b) as is shown for the PDZ-2. The pump-probe plots shows responses at Glu8 and Glu10 of 114.3 ± 11.7 and 120.6 ± 8.6 K,

respectively, when His86 is excited. Inversely, a response at His86 of 120.0 ± 12.6 K is observed when Glu10 is excited. A response at His86 of 115.4 ± 7.2 K is observed when Glu8 is excited (plot not shown). These measurements reinforce the idea of the presence of a symmetrical pump-probe relationship. The evaluation of the kinetic energy for the hydrogen-bonds for the interaction between Glu10 and HIS86 in three selected trajectories is shown figure 5d, e and f. In one side, when the pump is applied to Glu10 a kinetic energy of ~ 1500 J/mol at 10000 fs is observed for the Nitrogen atom of the N-H moiety of His86. These measurements a shows a higher value when compared to the kinetic energy analysis for Asp 5 (Figure 4) with a response of ~ 750 J/mol at 10000 fs for the Nitrogen atom of the N-H moiety of Lys91. In the other side, when His86 is excited similar kinetic patterns are observed with respect to the heat injection to Glu10. The comparison of the kinetic energy plots with the previous case Lys91-Asp5, support the idea of a symmetric response of the Glu10-His86 arrangement. The main difference in both cases relies in that the former form a charge assisted hydrogen bond with average length of ~ 2.62 Å (see insets in kinetic energy analysis Figure 5), while the latter form a non-charged hydrogen bond with average length of ~ 2.82 Å (see insets in kinetic energy analysis Figure 4). The enhancement of chemical reactivity of structural elements that surround hydrogen bonds that can suffer transition from normal bonding (> 2.8 Å) to short bonding regime (< 2.6 Å) has been previously reported (Mino, 2009). In line with this, the results of this report suggests that the heat diffusivity behavior, symmetric or asymmetric, may be modulated by length of the hydrogen bond.

The asymmetrical pump-probe relationship between His32 and Glu90 was also analyzed, for the ligand-free PDZ-2 model. These residues belong to pathway II. As shown in Figure 6a these residues are located in the loop connecting $\beta_2 - \beta_3$ and at the end of β_6 strand and a detail the representative snapshot of residues that are in contact with His32 and Glu90 is depicted in figure 6b. As can be observed in the detail of the thermal map (Figure 6c) there exists a preferential directionality of heat flow in which the heating of Glu90 has a increased pump to His32 than viceversa. The pump-probe plots of His32 and Glu90 (Figure 6d)

reveal an effective asymmetric relationship among these two residues. While the heating of Glu90 raises the local temperature of His32 up to 92.7 ± 17.2 K, the heating of His32, raises the local temperature of Glu90 to 74.5 ± 17.7 K. The observation of figure 6b directly explain the results of figure 6d. When the pump is applied at Glu90 the heat diffuses mainly to Arg57, His32 and Asp5. On the other side, when the pump is applied at His32 the heat diffuses to Arg57, Glu90. Due His32 has a contact with Glu67 in two alternating or simultaneous points (see Figure 6b) increased quantities of vibrational energy are transferred to it, thus, quenching the transference to Glu90. Here Glu67 is the most important heat sink, giving rise to the asymmetrical behavior. For these residues, this preferential directionality is observed in 19 of 20 samples obtained at the production stage, illustrates an example of directionality of signal propagation in proteins: a vibrational energy perturbation originated on Glu90 can be propagated to His32, but the opposite energy flow is much less intense.

Another example of heat transfer directionality was observed for the group of residues Lys13, Asn14, Asp15, Asn16 and Ser17 to Gln43 that is associated to Pathway I. Here, residues 13 to 17 readily transfer energy to Gln43, nevertheless Gln43 transfer preferentially to Asp15. Essentially, the only non-covalent heat sink of the Lys13-Ser17 sequence is Gln43, through the strong Asp15-Gln43 polar interaction. The structural motif, for the PDZ-2·L case, that results on this effect is shown in Figures 7a and b and the resulting thermal diffusion map shown in Figure 7c and pump probe plots are depicted in figure 7d. Residues 13 to 17 are located in the loop connecting $\beta_2 - \beta_6$, whereas residue Gln43 is located in the loop connecting $\beta_3 - \alpha_1$. The asymmetry of the response of Gln43 to Lys13-Ser17 heating relative to the response of these residues to the Gln43 heating is noticeable in Figure 7c. This asymmetric transfer is observed in PDZ-2 and is enhanced PDZ-2·L. A remarkable feature of the group 13 to 17 is formation of an hydrogen bond cluster which gives form a loop in this region. Between Asp 15 and Gln43, two HB are observed. The local three-dimensional organization of the residues forms a funnel-like structure pointing towards Gln43. This observations shows that heat is readily transferred through HB in the cluster and are useful to

explain the directionality of heat diffusion at this particular point in PDZ-2 and PDZ-2·L.

In summary, our results shows that it is possible to recover the information regarding pathway I and II using ATD. Also, our results suggest the important role of HB in vibrational coupling and signal directionality propagation and that topological characteristics of the contact network may give rise to signal transfer directionality.

Discussion and Conclusions.

Signal transduction in proteins is an important problem in structural biochemistry (Buchli et al. 2013, Cilia et al. 2012, Gerek and Ozkan, 2011). The aim of this particular work is to test one methodology, e.g. ATD, to identify asymmetric paths of energy propagation in the PDZ domain, and correlate it with allosteric mechanisms. This protein transfers allosteric signals with minor conformational changes and been cataloged as a Type I entropic allosteric system (Tsai et al., 2008). These Type of allosteric communication manifest in the alteration of the frequencies and amplitudes of residue fluctuations and involve several forms of dynamic behavior, from highly correlated, low-frequency normal-mode vibrations to random local anharmonic motions of individual groups or atoms. (Jusuf, 2003; Cooper and Dryden, 1984). Evidence from experimental (Fuentes et al.), statistical (Lockless et al, 1999) and theoretical (Erman, 2011; Kong and Karplus, 2009) studies support the same two allosteric pathways for PDZ-2. In Pathway I (See Figure 1) the allosteric communication goes from strand β_2 and extends along the long axis of the helix α_1 . Pathway II starts at strand β_2 and goes across strands β_3 , β_4 , β_6 to β_1 .

Our results demonstrate that PDZ-2 and PDZ-2·L have similar contact maps that resemble the thermal diffusion maps. We conclude that a correlation exists between the flow of vibrational energy, the cognate I and II allosteric pathways for PDZ-2 and PDZ-2·L and their respective contact maps. The presence of ligand can induce changes in the contact topology between secondary elements, so that

ligand can act as a modulator of the vibrational coupling of the allosteric pathways.

Our results shows that hydrogen-bonds are implicated in the heat flow among different segment of the protein as is shown in the case of the coupling between β_2 and α_2 . Here, hydrogen bonds formed between His71 and Thr23 for PDZ-2; and between His71 and Thr26 or between His71 and the C=O backbone moiety of Gly24 for PDZ-2·L. The role of hydrogen bonds in the enhancement of heat diffusion have been demonstrated in models of α -helices (Miño, 2014) in which a higher number of hydrogen-bonds produce higher thermalization rates in those structures. The role of hydrogen bonds in heat diffusion have also been demonstrated to occur in spider silk (Zang, 2014) So, our observations are consistent and supported by those previous reports.

The main result of our research is the detection of preferential heat flow directionality along allosteric pathways This directionality is evident from the observation of details the thermal maps for PDZ-2 and PDZ-2·L. The directionality occurs in absence of the ligand and can be modulated by its presence. This phenomena was studied at points of PDZ-2 and is consistent with the expected behavior of an allosteric protein, that is, to transfer signal with preferential directionality. The smallest organizational unit that present this property is the hydrogen-bond. Our punctual analysis of the interaction between Asp5 and Lys91 suggest that normal length hydrogen bonds behaves as thermal diode, that is, it transfer vibrational energy in preferential directionality. This effect may be originated from the specific force constants to describe the stretching of N-H and C=O moieties. While N-H is a single bond, C=O is a double bond, then the amplitude of the stretching that each moiety reach in front of similar thermal excitation is higher for the latter and lower for the former. Then the heat can be readily released from the N-H moiety by knocking out the Oxygen atom of the C=O moiety, but inverse excitation the C=O moiety required more energy to knock out the respective Hydrogen atom of the N-H moiety. The operation of hydrogen bonds as thermal diodes early have been described in molecular dynamics simulations of asymmetrical functionalized silica slabs floating in water

(Schoena, 2009). In those simulations one side of the silica is hydrophobic and the other side is hydrophilic, then the heat flow is favored when applied in the hydrophobic to hydrophilic direction and impeded in the inverse direction. In a smaller scale, our simulations, indicate that the heat flow is favored in the direction of $\text{N-H} \rightarrow \text{O=C}$ and impeded in the inverse direction in consistency with the report of Schoen et al. (2009). This behavior is compromised in the case of short hydrogen bonds, as is observed the pump-probe analysis of the interaction of Glu10-His86. As the Glu and His has -1 and +1 charge, respectively, both has the possibility of form short hydrogen bonds, $\sim 2.6 \text{ \AA}$. This is the main difference difference with respect to the interaction between Asp5-Lys91 that present a normal hydrogen-bond of length of $\sim 2.85 \text{ \AA}$. It seems that short distances between the N-H and the C=O moieties observed for the interaction between Glu10-His86 forbid the asymmetric behavior of thermal diffusion. It has been previously shown, by quantum mechanical models, that the transition between normal to short bonding regime significantly alters the chemical reactivity of the structural elements that surround the given hydrogen bond (Miño,2009). Here, we suggest, using classical molecular dynamics that the transition between normal to short hydrogen bond regime may modulate the thermal diode effect shown by hydrogen bonds.

Also, asymmetrical heat transference is observed in complex interaction of residues as is depicted for Figures 6 and 7. In the case of the asymmetrical pump-probe relationship between Glu90-His32 a set of hydrogen bonded interacting residues explain the observed directionality. For example, when heat is provided to Glu90, it is directly transfered to His32, Arg57 and to Asp5, while the structural organization that surround His32, namely, Gly33 and Glu67, quenches the heat transfer to Glu90. Here, as is shown in the pump-probe plot of His32, Glu67 acts as a thermal sink that trapping an important quantity of heat. So, the topological organization of a set of interacting residues may be the reason of an asymmetrical heat diffusion behavior. A similar phenomenology seems to be operative in the interaction of the residues 13 to 17 and Gln43 (Figure 7). The

observation of the structure at this segment reveals an hydrogen bond network organization similar to a funnel pointing towards residue Gln43. As the residues 13 to 17 are heated they distribute heat among each other, and transfer to Gln43, while the heating of Gln43 transfer back mainly to residue Asp15 which is the individual heat connection of group 13 to 17 to Gln43. All the previous facts suggest an important role of hydrogen bonds for vibrational coupling among segments of secondary structure in this system and hence in the constitution of the allosteric pathways.

In summary, in this work we have analyzed the vibrational energy diffusion in PDZ-2 and the correlation with cognate allosteric pathways for this system. Also we offer examples of asymmetrical heat propagation in protein structures that gives rise to signal directionality. The ATD analysis is consistent with experimental (Fuentes et al.), statistical (Lockless et al, 1999) and theoretical (Erman, 2011; Kong and Karplus, 2009) methods previously used to characterize and define the allosteric pathways I and II for this system. Thermal diffusion maps show a high degree of correspondence with connectivity maps supporting the idea that for Type I allosteric communication it is the connectivity network that defines the allosteric route and its directionality.

References.

- Boxus M, Twizere JC, Legros S, Dewulf JF, Kettmann R, Willems L (2008). The HTLV-1 Tax interactome. *Retrovirology* 5: 76.
- Buchli B, Waldauer SA, Walser R, Donten ML, Pfister R, Blöchliger N, Steiner S, Caflisch A, Zerbe O, Hamm P. (2013) Kinetic response of a photoperturbed allosteric protein. *Proc Natl Acad Sci U S A*.110:11725-30.
- Burendahl S, Nilsson L.(2012) Computational studies of LXR molecular interactions reveal an allosteric communication pathway. *Proteins*. 80:294-306.
- Cilia E, Vuister GW, Lenaerts T. (2012) .Accurate prediction of the dynamical changes within the second PDZ domain of PTP1e. *PLoS Comput Biol*. 2012;8(11):e1002794.

Cooper A, Dryden DT.(1984) Allostery without conformational change. A plausible model. *Eur Biophys J.* 11(2):103-9.

Erman, B. (2011) Relationship between ligand binding sites, protein architecture and correlated paths of energy and conformational fluctuations. *Phys. Biol.* 8 : 0560003

Fuentes EJ, Gilmore SA, Mauldin RV, Lee AL. (2006) Evaluation of energetic and dynamic coupling networks in a PDZ domain protein. *J Mol Biol.* Dec 1;364(3):337-51.

Frauenfelder, H., McMahon, B. H., Austin, R. H., Chu, K. & Groves, J. T. (2001). The role of structure, energy landscape, dynamics, and allostery in the enzymatic function of myoglobin. *Proc. Natl Acad. Sci. USA*, 98, 2370– 2374.

Gerek ZN, Ozkan SB.(2011) Change in allosteric network affects binding affinities of PDZ domains: analysis through perturbation response scanning. *PLoS Comput Biol.* 2011 Oct;7(10):e1002154.

Gutierrez G, Menendez-Proupin E, Loyola C, Peralta J, Davis S (2010) Computer simulation study of amorphous compounds: structural and vibrational properties. *J Mater Sci* 45:5124–5134

Green, S. M. & Shortle, D. (1993). Patterns of non-additivity between pairs of stability mutations in *Staphylococcal nuclease*. *Biochemistry*, 32, 10131–10139.

Jusuf S, Loll PJ, Axelsen PH (2003) Configurational entropy and cooperativity between ligand binding and dimerization in glycopeptide antibiotics. *J Am Chem Soc* 125:3988–3994.

Kong Y, Karplus M.(2009)Signaling pathways of PDZ2 domain: a molecular dynamics interaction correlation analysis.*Proteins.* Jan;74(1):145-54.

Koshland DE, Nemethy G, Filmer D (1966) Comparison of Experimental Binding Data and Theoretical Models in Proteins Containing Subunits. *Biochemistry*;5:365.

Humphrey W, Dalke A, Schulten K (1996) VMD—visual molecular dynamics. *J Mol Graph* 14:33–38

Laine E, Auclair C, Tchertanov L.(2012) Allosteric communication across the native and mutated KIT receptor tyrosine kinase.*PLoS Comput Biol.* 2012;8(8):e1002661.

Liu J, Tawa GJ, Wallqvist A. (2013) Identifying cytochrome p450 functional networks and their allosteric regulatory elements. PLoS One. 8(12):e81980.

Leitner DM. (2008) Energy flow in proteins. Annu Rev Phys Chem. 59:233-59.

Leitner DM. (2009) Frequency-resolved communication maps for proteins and other nanoscale materials. J Chem Phys. 2009 May 21;130(19):195101.

Lockless S, Ranganathan R (1999). Evolutionarily conserved pathways of energetic connectivity in protein families. Science. 286:295.

Mace, J. E., Wilk, B. J. & Agard, D. A. (1995). Functional linkage between the active site of alpha-lytic protease and distant regions of structure: scanning alanine mutagenesis of a surface loop affects activity and substrate specificity. J. Mol. Biol. 251, 116 – 134.

Martínez, L.; A. C. M. Figueira, I. Polikarpov, M. S. Skaf. (2011) Mapping the Intramolecular Vibrational Energy Flow in Proteins Reveals Functionally Important Residues. J. Phys. Chem. Lett. 2, 16, 2073-2078.

MackKerell AD Jr, Bashford D, Bellott M, Dunbrack RL Jr, Evanseck J, Field MJ, Fischer S, Gao J, Guo H, Ha S, Joseph D, Kuchnir L, Kuczera K, Lau FTK, Mattos C, Michnick S, Ngo T, Nguyen DT, Prodhom B, Reiher IWE, Roux B, Schlenkrich M, Smith J, Stote R, Straub J, Watanabe M, Wiorkiewicz-Kuczera J, Yin D, Karplus M (1998) All-atom empirical potential for molecular modeling and dynamics studies of proteins. J Phys Chem B 102:3586–3616

Meroueh, S. O., Roblin, P., Golemi, D., Mavegraud, L., Vakulenko, S. B., Zhang, Y. et al. (2002). Molecular dynamics at the root of expansion of function in the M69L inhibitor-resistant TEM beta-lactamase from Escherichia coli. J. Am. Chem. Soc. 124, 9422– 9430.

Miño, G. Barriga, R. and Gutierrez, G. Hydrogen Bonds and Heat Diffusion in α -Helices: A Computational Study. 2014 Aug 28;118(34):10025-34.

Monod J, Wyman J, Changeux JP. (1965) On Nature of Allosteric Transitions - a Plausible Model. J Mol Biol 2:88.

Noinaj N, Bhasin SK, Song ES, Scoggin KE, Juliano MA, Juliano L, Hersh LB, Rodgers DW.(2011)Identification of the allosteric regulatory site of insulysin. PLoS One. 2011;6(6):e20864.

Ota N, Agard DA (2005) Intramolecular signaling pathways revealed by modeling anisotropic thermal diffusion. J Mol Biol 351: 345–354

Olsen, D. B., Stahlhut, H. W., Rutkowski, C. A., Schock, H. B., van Olden, A. L. &

Kuo, L. C. (1999). Non-active site changes elicit broad-based cross-resistance of the HIV-1 protease to inhibitors. *J. Biol. Chem.* 274, 23699– 23701.

Popovych N, Sun SJ, Ebright RH, Kalodimos CG. (2006) Dynamically driven protein allostery. *Nat Struct Mol Biol*; 13:831–838.

Ponting CP (February 1997). "Evidence for PDZ domains in bacteria, yeast, and plants". *Protein Sci.* 6 (2): 464–468. doi:10.1002/pro.5560060225. PMC 2143646. PMID 9041651.

Rod, T. H., Radkiewicz, J. L. & Brooks, C. L., III (2003) Correlated motion and the effect of distal mutations in dihydrofolate reductase. *Proc. Natl Acad. Sci. USA*, 100, 6980– 6985.

Seldeen KL, Deegan BJ, Bhat V, Mikles DC, McDonald CB, Farooq A.(2011) Energetic coupling along an allosteric communication channel drives the binding of Jun-Fos heterodimeric transcription factor to DNA.*FEBS J.* 2011 Jun;278(12):2090-104

Schoen, P. A. E.; Michelb, B.; Curionib, A.; Poulikakosa, D.Hydrogen-bond enhanced thermal energy transport at functionalized,-hydrophobic and hydrophilic silica–water interfaces. *Chem. Phys. Lett.* 2009, 476, 271–276.

Tsai CJ, Del Sol A, Nussinov R. *J Mol Biol.* (2008) Allostery: absence of a change in shape does not imply that allostery is not at play. *Apr 18*;378(1):1-11

Zhang, L.; Chen, T.; Bana, H.; Liu, L. Hydrogen bonding-assisted thermal conduction in β -sheet crystals of spider silk protein. *Nanoscale* 2014, 6, 7786–7791

Voet D, Voet J (1995) *Biochemistry*, 2nd edn. Wiley, New York

Figures and Captions.

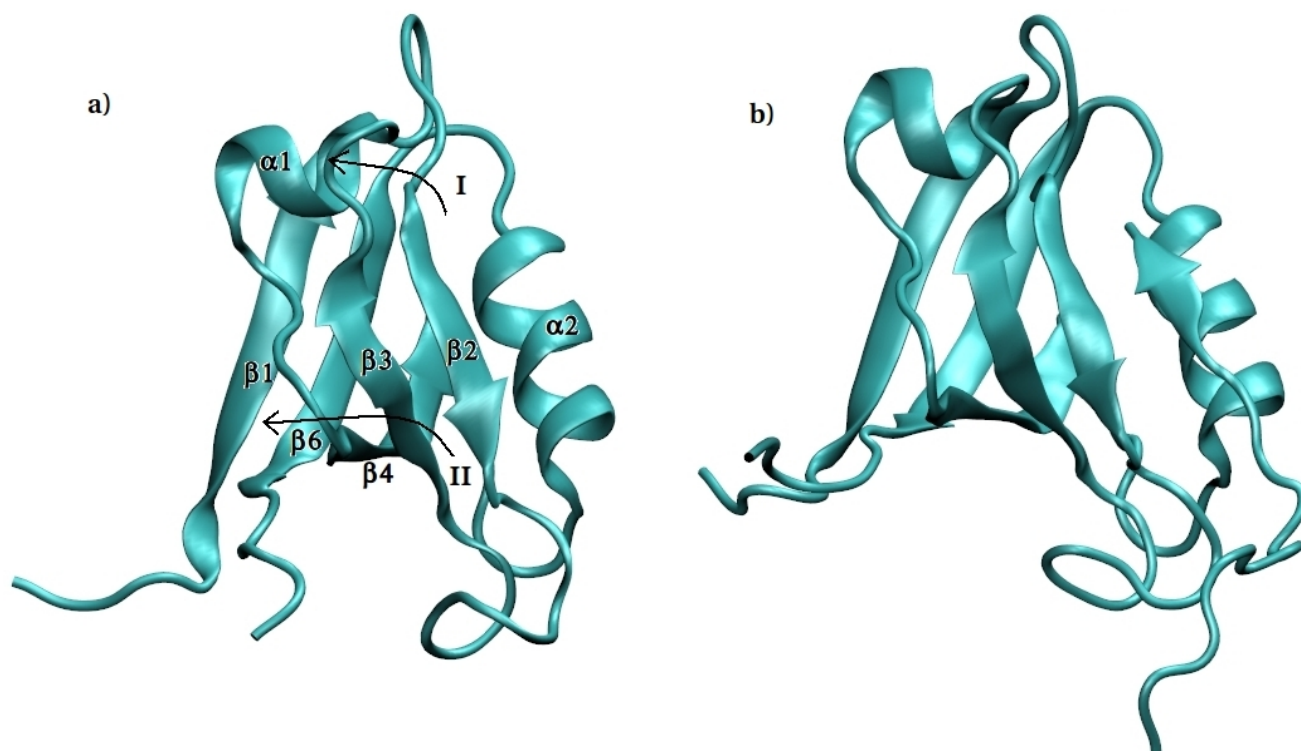
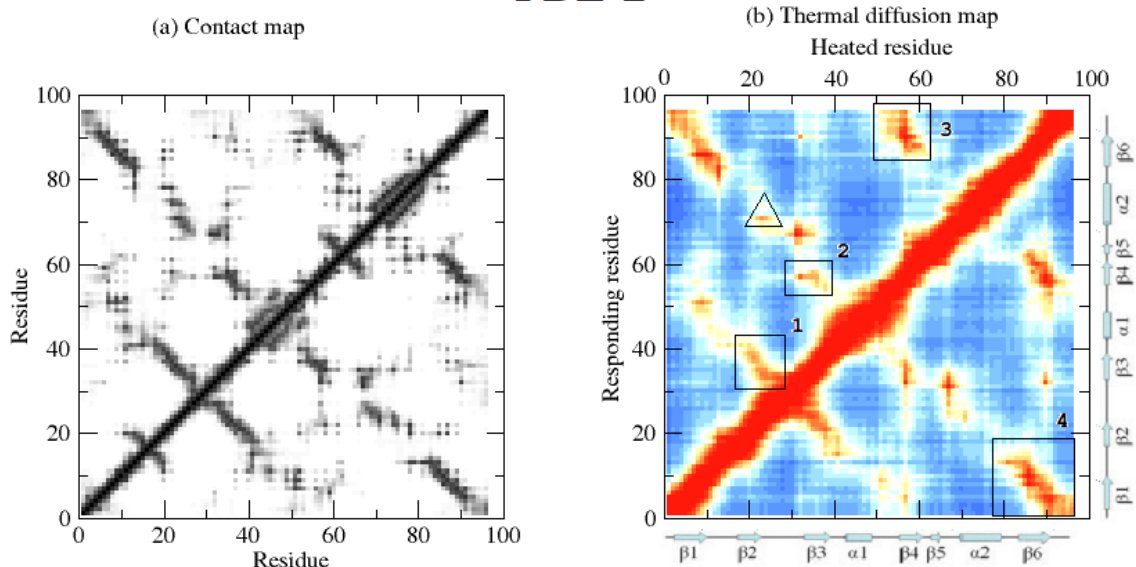


Figure 1. PDZ-2 with (a) and without ligand (b). In (a) the proposed pathways I and II are depicted. Beta sheet 5 is located behind $\beta 2$ in both images.

PDZ-2



PDZ-2·L

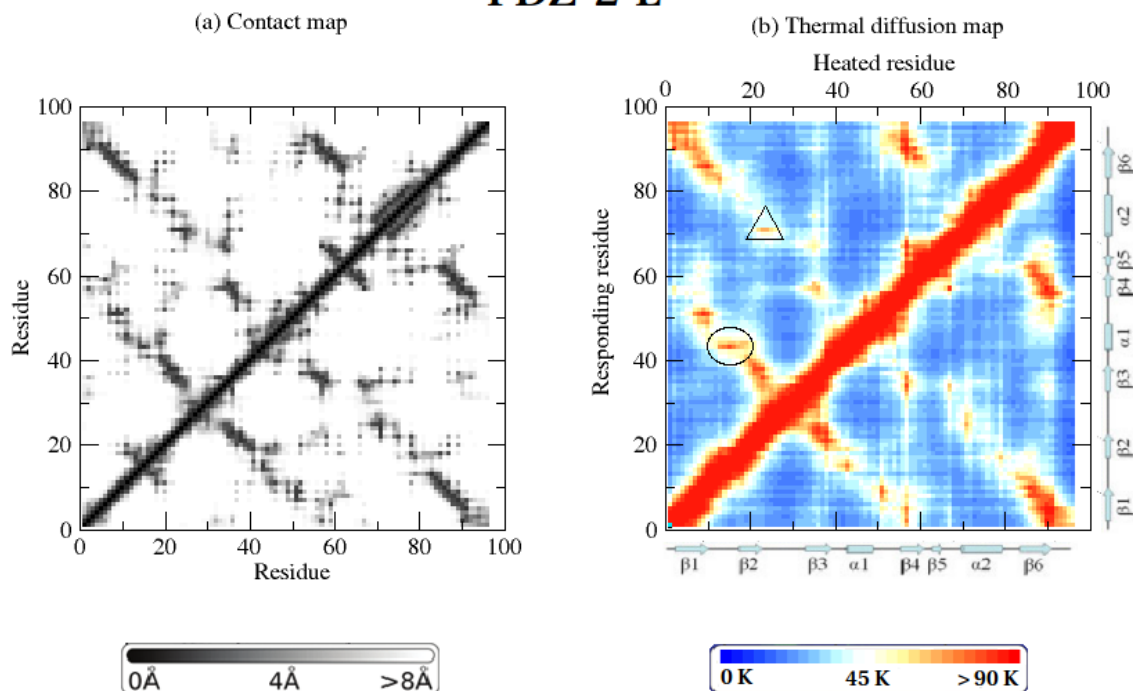


Figure 2. Average contact (a) and thermal diffusion map (b) for PDZ-2 and PDZ-2·L ($n=20$). Boxes 1, 2, 3 and 4 represent coupling associated to pathway II, circle represent coupling associated to pathway and triangle represent a case of heat transference mediated by HB (see figure 3 and text for further details)

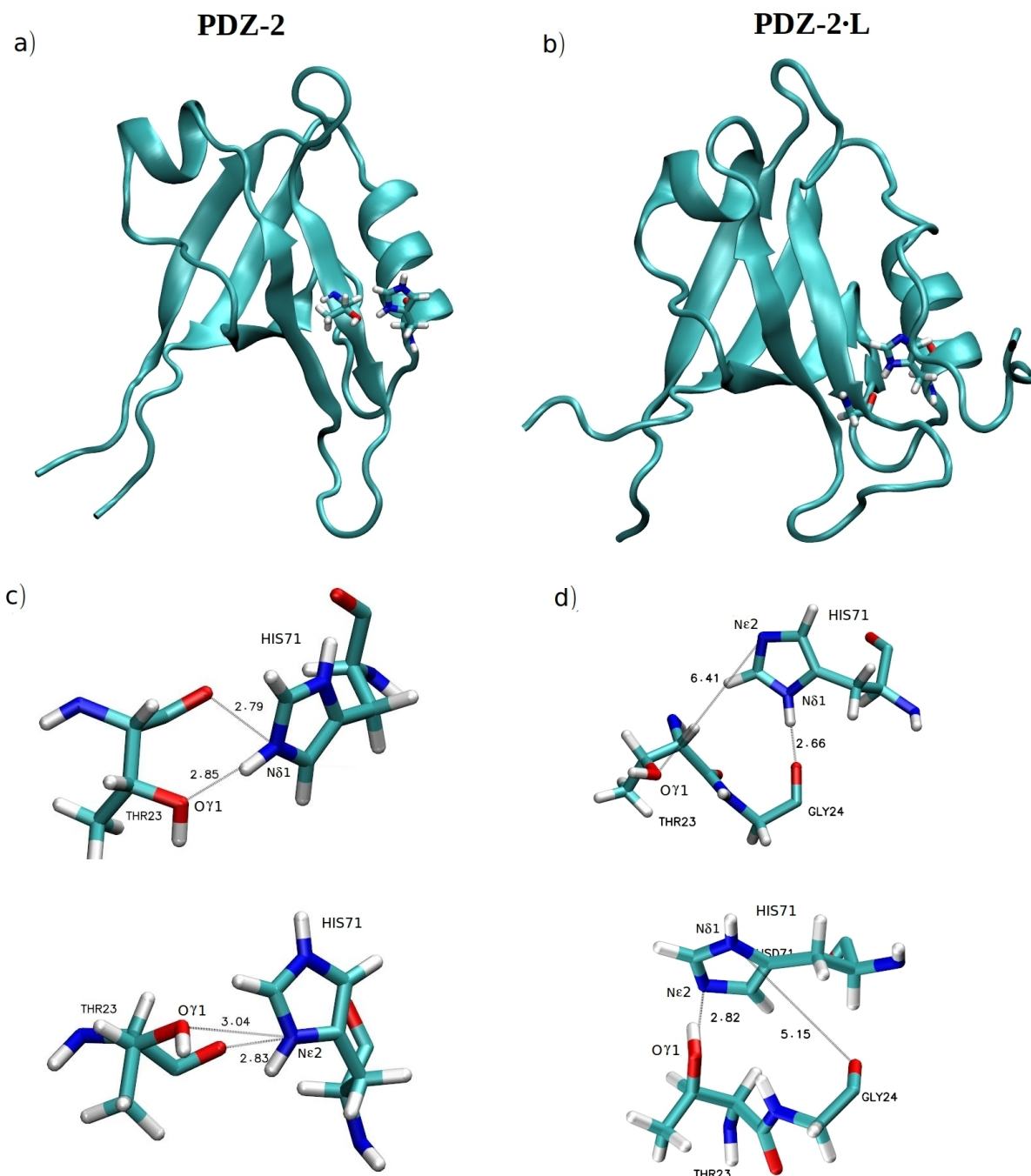


Figure 3. Snapshots of interaction for PDZ-2 (a) and PDZ-2·L (b) and details of the respective hydrogen bond interactions between His71-Thr23 (c) and His71-Thr23-Gly24 (d) that give rise to β_2 and α_2 coupling in each case.

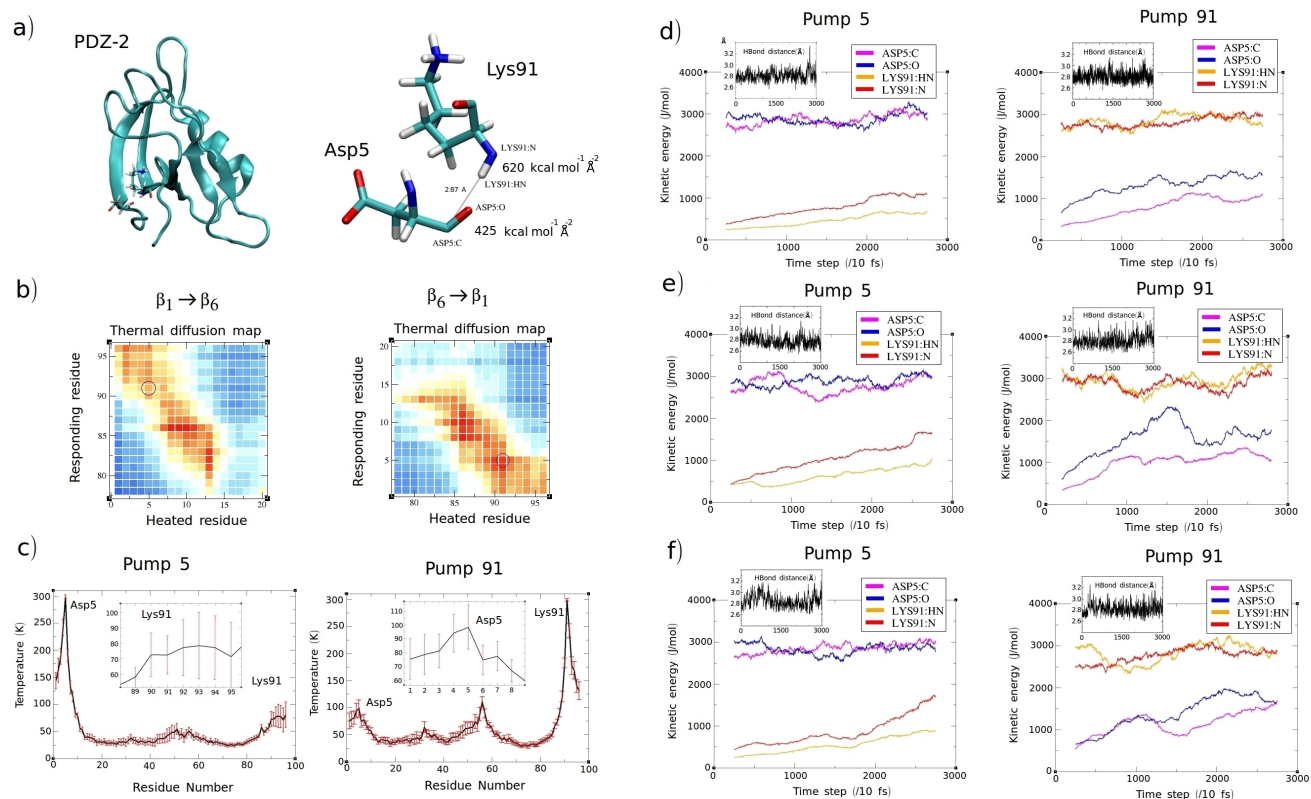


Figure 4. (a) Snapshot of Asp5-Lys91 interaction in PDZ-2 case. (b) Details of thermal maps for segments β₁ - β₆. (c) Pump probe plots of Asp5 and Lys91 (n=20). (d,e,f) Kinetic analysis per atom plotted using a running average of 250 time steps. Insets represents hydrogen bond distance versus time step for Lys91-N-H...O=C-Asp5 interaction (see text for details).

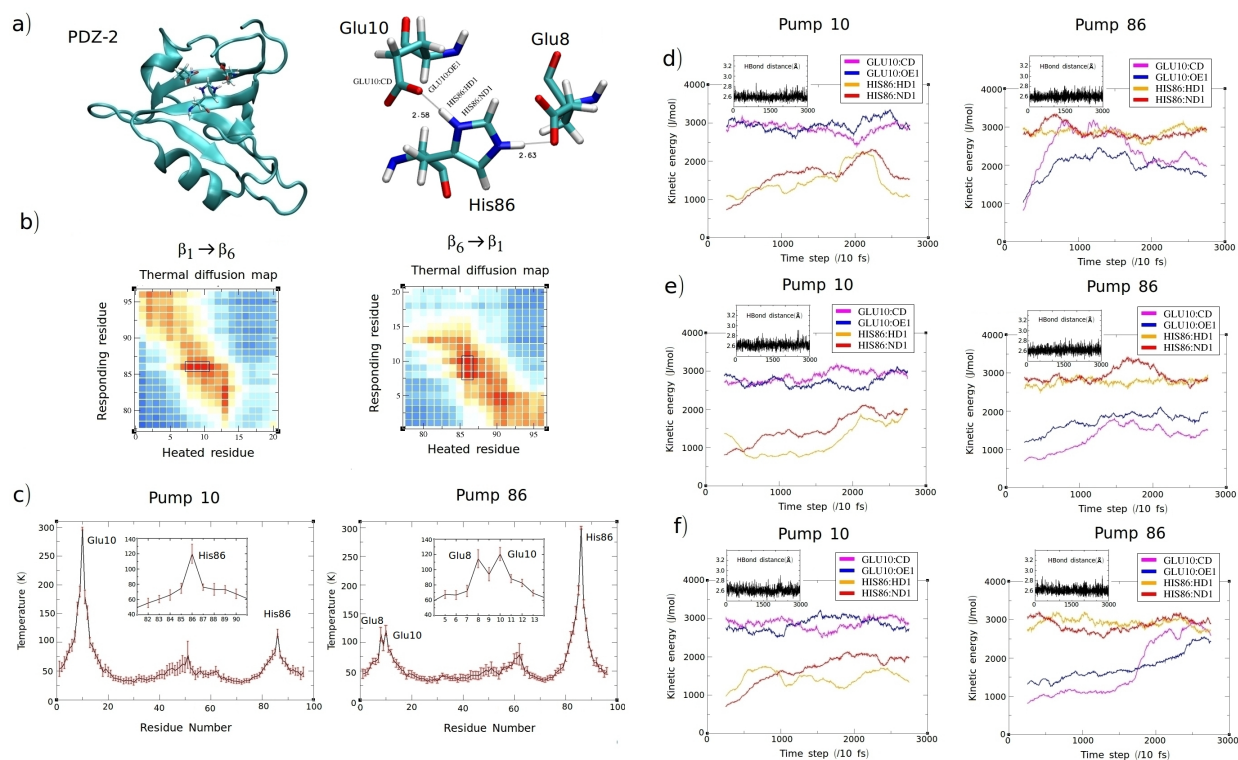


Figure 5. (a) Snapshot of Glu10-His86 interaction in PDZ-2 case. (b) Details of thermal maps for segments $\beta_1 - \beta_6$. (c) Pump probe plots of Glu10 and His86 ($n=20$). (d,e,f) Kinetic analysis per atom plotted with using a running average of 250 time steps. Insets represents hydrogen bond distance versus time step for His86-N-H \cdots O=C-Glu10 interaction (see text for details).

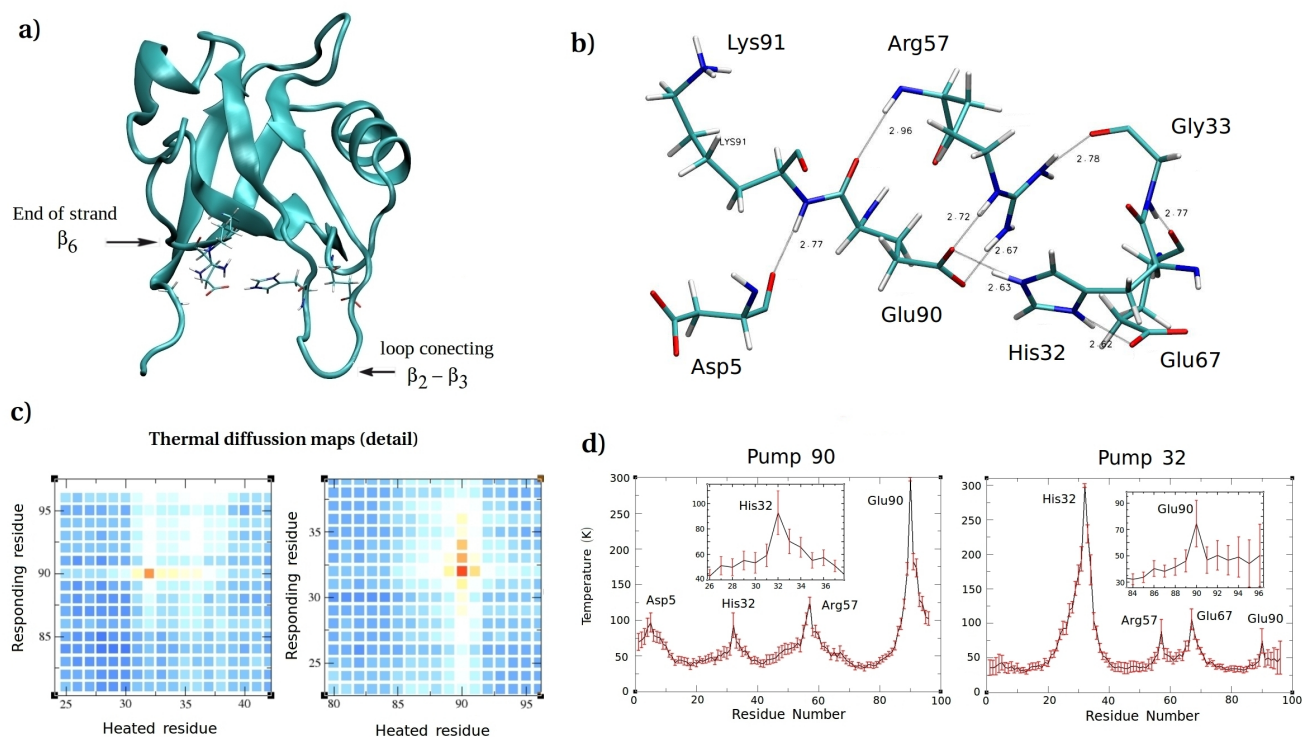


Figure 6. a) Structural location of residues Gly5, His32, Arg57, Glu67 and Glu90 in PDZ-2. b) Two details of two (i, ii) relative orientation of the residues. c) Detail of thermal diffusion maps for the asymmetrical relationship between Glu90 and His32 ($n=20$). d) Averaged Pump-probe of Glu90 and His32.

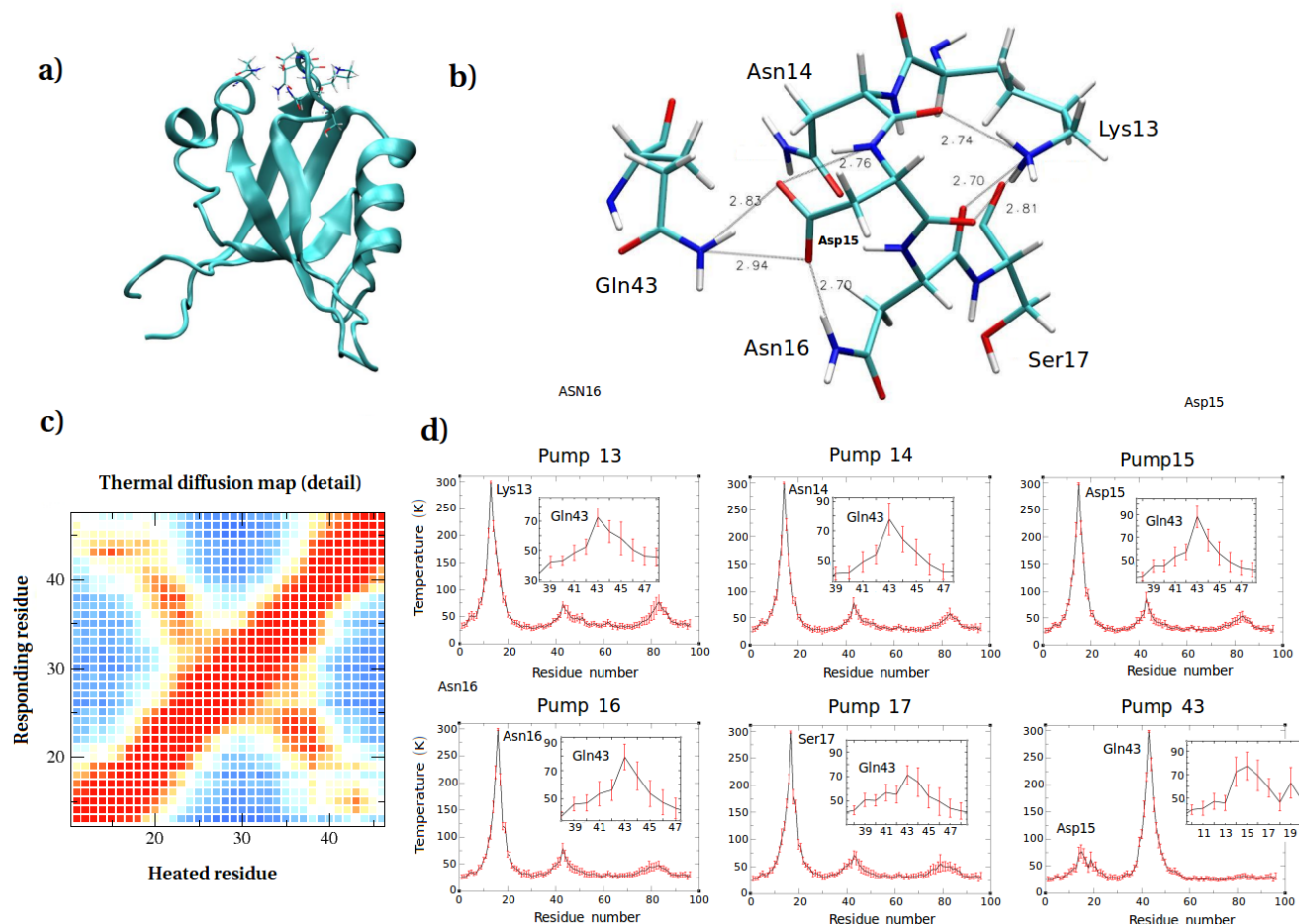


Figure 7. a) Structural location of residues Lys13, Asn14, Asp15, Asn16, Ser17 and Gln43 in PDZ-2·L. b) Detail of the positions of those residues with Hydrogen bond distances in Angstroms. c) Detail of the thermal map of PDZ-2·L for the section involving pathway I. d) Pump probe relation for the involved residues (n=20).